Atmospheric
Chemistry
and Physics
Discussions

Volatility measurement of atmospheric submicron aerosols in an urban atmosphere in southern China

Li-Ming Cao[1], Xiao-Feng Huang[1], Yuan-Yuan Li[1], Min Hu[2], Ling-Yan He[1]

[1]Key Laboratory for Urban Habitat Environmental Science and Technology, School of Environment and Energy, Peking
University Shenzhen Graduate School, Shenzhen, 518055, China
[2]State Key Joint Laboratory of Environmental Simulation and Pollution Control, College of Environmental Sciences and
Engineering, Peking University, Beijing, 100871, China

Correspondence to: Xiao-Feng Huang (huangxf@pku.edu.cn)

Abstract. Aerosol pollution has been a very serious environmental problem in China for many years. The volatility of aerosols
can affect the distribution of compounds in the gas and aerosol phases, the atmospheric fates of the corresponding components
and the measurement of the concentration of aerosols. Compared to the characterization of chemical composition, few studies
have focused on the volatility of aerosols in China. In this study, a TD-AMS (Thermo-Denuder – Aerosol Mass Spectrometer)
system was deployed to study the volatility of non-refractory PM_1 species during winter in Shenzhen. To our knowledge, this
paper is the first report of the volatilities of aerosol chemical components based on a TD-AMS system in China. The average
PM_1 mass concentration during the experiment was 42.7 ± 20.1 μg m^{-3}, with organics being the most abundant component
(43.2% of the total mass). The volatility of chemical species measured by the AMS varied, with nitrate showing the highest
volatility, with an MFR (mass fraction remaining) of 0.57 at 50 °C. Organics showed semi-volatile characteristics (the MFR
was 0.88 at 50 °C), and the volatility had a relatively linear correlation with the TD temperature (from 50 to 200 °C), with an
evaporation rate of 0.45 %·°C^{-1}. Five subtypes of OA were resolved from total OAs by PMF for data obtained under both
ambient temperature and high temperatures through the TD, including a hydrocarbon-like OA (HOA, accounting for 13.5%),
a cooking OA (COA, 20.6%), a biomass burning OA (BBOA, 8.9%) and two oxygenated OAs (OOA): a less-oxidized OOA
(LO-OOA, 39.1%) and a more-oxidized OOA (MO-OOA, 17.9%). Different OA species presented different volatilities; the
volatility sequence of OA factors at 50 °C was HOA (MFR of 0.56) > LO-OOA (0.70) > COA (0.85) ≈ BBOA (0.87)> MO-
OOA (0.99). The volatility sequence of OA components suggested that HOA, rather than BBOA or COA, could be a potentially
important source of LO-OOA through the oxidizing process of "Evaporation – Oxidation in gas phase - Condensation". The
results above can contribute to the understanding of the formation and ageing of submicron aerosols in the atmosphere and
will help to constrain aerosol modelling inputs.

Introduction

Atmospheric aerosol pollution has important impacts on climate change, visibility and human health (Bohnenstengel et al.,
2014; Baklanov et al., 2015). Aerosols can be emitted, naturally or anthropogenically, by primary sources or produced by

secondary chemical reactions from gaseous precursors (IPCC, 2013). Volatility is one of the most important properties of aerosols, as it can determine the gas-particle phase partitioning of aerosols directly. The saturation vapour pressure, which is affected by temperature and vaporization enthalpies as described by the Clausius-Clapeyron equation, is the main factor that dominates the gas-particle phase partitioning of compounds. Volatility can be determined by the saturation vapour pressure or

5   saturation concentration, while the deposition rates of aerosols for wet or dry deposition are greatly influenced by the phase of aerosols (Bidleman, 1988). The chemical mechanism and reaction rates of gas, liquid and heterogeneous reactions can also result in a great difference because of the phase, the concentration and the lifetime of aerosols can also be influenced (Huffman et al., 2009a). The volatility of organic aerosols (OAs) also contributes greatly to the uncertainty in predicting the atmospheric aerosol concentration (Donahue et al. 2006; Pankow and Barsanti 2009). Since OAs contribute 30-80% of total aerosol mass

10   according to previous studies (Hallquist et al., 2009; Zhang et al., 2007a), further research regarding the volatility of atmospheric aerosols, especially organic aerosols, is very important in the understanding of aerosol characterization and source apportionment. Some previous studies examined several kinds of OA emission sources, including traffic emissions, combustion sources and the oxidation of primary OAs, and showed differences in volatility according to their different compositions (Huffman et al., 2009a; Xu et al.,2016; Paciga et al., 2016).

15   A thermo-denuder (TD) is a device that is widely used to estimate aerosol volatility distributions (Wehner et al., 2002; An et al., 2007; Huffman et al., 2008; Xu et al., 2016). The residence time of aerosols in TDs has been proven to affect the evaporation dynamics and kinetics (Saleh et al., 2008; Faulhaber et al., 2009). The TDs designed by Burtscher et al., 2001 and Wehner et al., 2002 typically are operated under temperatures higher than 200 °C and have average residence times from 0.3 to 9 s, focusing on very low volatility species. An et al., 2007 and Huffman et al., 2008 developed TDs with longer residence times

20   to make them more suitable for measuring the volatility of semi-volatile organic aerosols. An et al., 2007 studied the volatility of $(NH_4)_2SO_4$ and SOA produced by α-pinene/O_3 reaction and by α-pinene/NOx photo-oxidation and identified the volatility characteristics of SOA. The combined TD and Aerodyne Aerosol Mass Spectrometer (TD-AMS) system has been applied in many field and laboratory studies (Huffman et al., 2008; Huffman et al., 2009a and b; Lee et al., 2010). Hu et al., 2016 investigated the volatility of IEPOX-SOA with TD-AMS, showing that the volatility distribution of IEPOX-SOA was much

25   lower than those of the monomer tracers that have been reported as the major components of its mass.

Aerosol pollution has been one of the most important air quality problems in China. Many studies focused on aerosol source apportionment and chemical and physical properties have been carried out in most of the regions in China, especially in the Yangtze River Delta Region, the Pearl River Delta Region and the Beijing-Tianjin-Hebei Region in the past few years (Huang et al 2010, 2012, 2013; He et al., 2011). However, the volatility of aerosols is rarely researched in China currently. Bi et al.,

30   2015 studied the single–particle volatility of elemental carbon (EC) particles in the PRD region and showed that the volatility of EC-containing particles depends on the types of EC particles.

In this paper, the TD-AMS system was first deployed to determine the volatilities of non-refractory PM_1 species in China. With the high-resolution mass spectra of organics, the volatilities of OAs from different sources and their implications for organic aerosol ageing were also explored.

Experimental methods

5   ### 2.1 Sampling site description

Shenzhen (113.9°E, 22.6°N) is located on the southeast coast of China, in the southeast corner of the Pearl River Delta region with Hong Kong neighbouring to the south and Dongguan (a famous industrial city in China) to the north. The climate in Shenzhen is a subtropical oceanic climate that is deeply influenced by monsoon. The sampling site was located on the campus of Shenzhen Graduate School, Peking University in the western urban area of Shenzhen. The area surrounding the sampling

10   site was mostly covered by subtropical plants, and there was only a local road that was approximately 100 m away, which can be regarded as an anthropogenic emission source. The measurement was taken from 31 December 2014 to 23 January 2015 in winter, which is the season with the highest air pollution due to regional transportation from northwest and northeast China. The average ambient temperature was 15.9 ± 4.2 °C, and the relative humidity was 62.9 ± 17.5 %. The wind was mostly from the northeast and northwest with an average speed of 0.8 ± 0.7 m/s.

15   ### 2.2 Description of the thermo-denuder (TD) and HR-ToF-AMS

The aerosol volatility measurements were conducted with a TD – AMS system. The thermo-denuder and the high resolution time-of-flight aerosol mass spectrometer (HR-ToF-AMS, referred to hereafter as AMS) were both manufactured by Aerodyne Research Inc., US. The principle theory of an AMS can be found in previous studies (DeCarlo et al., 2006; Canagaratna et al., 2007). The TD used in this experiment is based on the design of Huffman et al., 2008. It consists of two parts: the heating

20   section and the denuder section. The stainless steel heating section is 22.25 inches (56.5 cm) in length with a 1-inch OD (2.5 cm) and a 0.875-inch ID (2.2 cm), wrapped with three fibreglass-coated heating tapes. The heating section is then joined to a 22-inch (56 cm) denuder section. The denuder section is filled with activated charcoal at room temperature to adsorb the gas phase species evaporated from particles. The temperature in the heating section was set at 48, 95, 143 and 192 °C to make the real temperature at the centreline, measured with a thermocouple, reach 50, 100, 150 and 200 °C, respectively. The TD was

25   placed upstream of the AMS. The aerosol flow can go through the heating and denuder sections (TD path) before being sampled by the AMS or flowing directly (ByPass path) into the AMS. The residence time of aerosols in the heating section was approximately 27.9 s with a flow rate of 0.45 L/min. The AMS was set with 4 menus: ByPass path in V-mode, TD path in V-mode, TD path in W-mode and ByPass path in W-mode.

2.3 Particle Loss Correction

The particle losses through the TD should be of concern for quantitative measurements with the TD, as it can decrease the transmission efficiency through the TD. There are three mechanisms of particle loss inside the TD: sedimentation, thermophoretic and diffusional processes (Burtscher et al., 2001; Wehner et al., 2002). Burtscher et al., 2001 determined that the dominant effects would be determined by the temperature and particle size: sedimentation increases as the particle size increases and would be negligible when the TD is vertical; diffusive losses increase with decreasing particle size; and thermophoresis is not strongly dependent on particle size, is important in the denuder section and will partly compensate for diffusion in the heating section.

The transmission efficiency in this research was calculated via an experiment. CsCl solution was atomized and then measured by DMA/CPC before and after the TD. The transmission efficiency of the ByPass path was regarded as 1. The average transmission efficiency through the TD is approximately 90%, at 50, 100, 150 and 200 °C, as shown in Figure 1, which is similar to previous studies (Huffman et al., 2008; Xu et al., 2016).
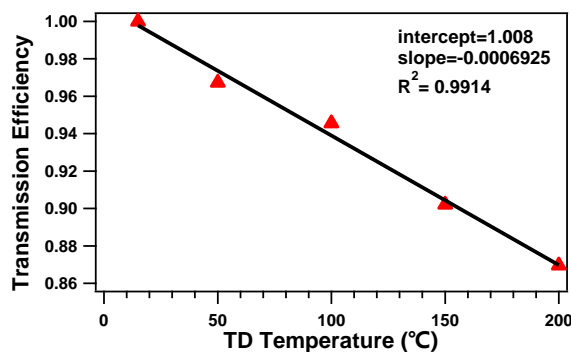

Figure 1. Temperature related transmission efficiency through the TD.

2.4 Source Apportionment Method

Positive matrix factorization (PMF) was applied to the high resolution organic mass spectra using the PMF evaluation tool developed by Ulbrich et al., 2009. The data and error matrix were processed according to the signal-to-noise ratio (SNR) as reported in previous papers (Ulbrich et al., 2009; Huang et al., 2010; He et al., 2011). Weak ions ($0.2 < SNR < 2$) were downweighted by a factor of 2, bad ions ($SNR < 0.2$) were removed from the analysis (Paatero and Hopke, 2003), and CO_2^+ related ions (O^+, HO^+, H_2O^+ and CO^+) were also downweighted (Ulbrich et al., 2009).

The PMF analysis was based on the full high-resolution organic dataset (data sampled both under ambient temperature and pre-processed by the TD) for 1 to 10 factors with fpeak varying from -1 to 1 (seed), increasing with a step of 0.1, and seed

Atmospheric
Chemistry
and Physics
Discussions

varying from 0 to 250 (fpeak = 0) in steps of 10. The diagnostic plots of the solutions are shown in Figure S1 in the supplement, including the $Q/Q_{expected}$ ratio, the characteristics of the different mass spectra, the scaled residuals, and the correlation of the component time series with the external tracers. The solutions with more than five factors showed no distinct information but splitting of the factors; the $Q/Q_{expected}$ showed the lowest value at fpeak=0; the varied fpeak did not improve the results; and

5   the varied value of seed also made no significant difference of the solution. Therefore, the solution of five factors, fpeak = 0 and seed = 0, was determined as the optimal solution for this experiment, and the five factors are hydrocarbon-like organic aerosol (HOA), cooking organic aerosol (COA), biomass burning organic aerosol (BBOA), less-oxidized oxygenated organic aerosol (LO-OOA) and more-oxidized oxygenated organic aerosol (MO-OOA).

As discussed by Huffman et al., 2009, the PMF solution of all data points collected both with and without pre-processing by

10   the TD could facilitate the separation of different factors by enhancing the contrast of the time series of these factors. On the other hand, it could also introduce additional variability in the MS and distort the PMF fit. The result of SOAR-1 and MILAGRO datasets showed that the PMF solution for the TD-AMS data could successfully recover the factors resolved with data sampled only under ambient temperature, and it was recommended by Huffman et al., 2009 to use TD-AMS data while performing PMF analysis. Xu et al., 2006 also discussed the difference in the PMF solution between the two methods and

15   encountered a mixing behaviour of OA factors in PMF analyses that included data with TD pre-processing. Therefore, the PMF results with data obtained only under ambient temperature were also explored and the best solution was presented in Figure S2 in the supplement. Compared to the previous results including TD pre-processed data, the HOA and OOA were mixed to some extent. Therefore, the PMF solution with the inclusion of TD pre-processed data was identified as the final results.

3 Results and discussion

3.1 PM$_1$ chemical compositions

Figure 2a shows the time series of the mass concentration of non-refractory species measured by the AMS and black carbon measured with an Aethalometer (AE-31, Magee, US) during the experiment. Apart from when the mass concentration of all the PM$_1$ species decreased markedly due to rain during 12 and 13 January, sulfate showed a relatively stable time series

25   compared to the other species, indicating that sulfate was mainly influenced by regional transportation, while other species, such as organics, nitrate, chloride and black carbon (BC), were significantly affected by local emission sources. The sum of the species measured with the AMS and with the aethalometer was regarded as PM$_1$, which showed a high correlation (R^2=0.94, slope=1.1, in Figure S3) with the mass concentration derived from the particle number concentration between 15 and 600 nm measured by a collocated scanning mobility particle sizer (SMPS, TSI Inco.) by assuming the densities of the components

30   obtained in the literature (Kuwata et al., 2012; Poulain et al., 2014; Hu et al., 2017). In result, the average mass concentration of PM$_1$ was 42.7 ± 20.1 µg m^{-3}, ranging from 3.9 to 134.1 µg m^{-3}, while organics were the most abundant PM$_1$ component,

contributing 43.2% to the total PM$_1$ mass concentration, followed by sulfate (21.2%), black carbon (12.2%), nitrate (11.4%), ammonium (10.4%) and chloride (1.6%). The measured and predicted ammonium showed a high correlation (R^2=0.97) with a slope of 0.85, implying that the aerosols showed some acidity (Zhang et al., 2007b).
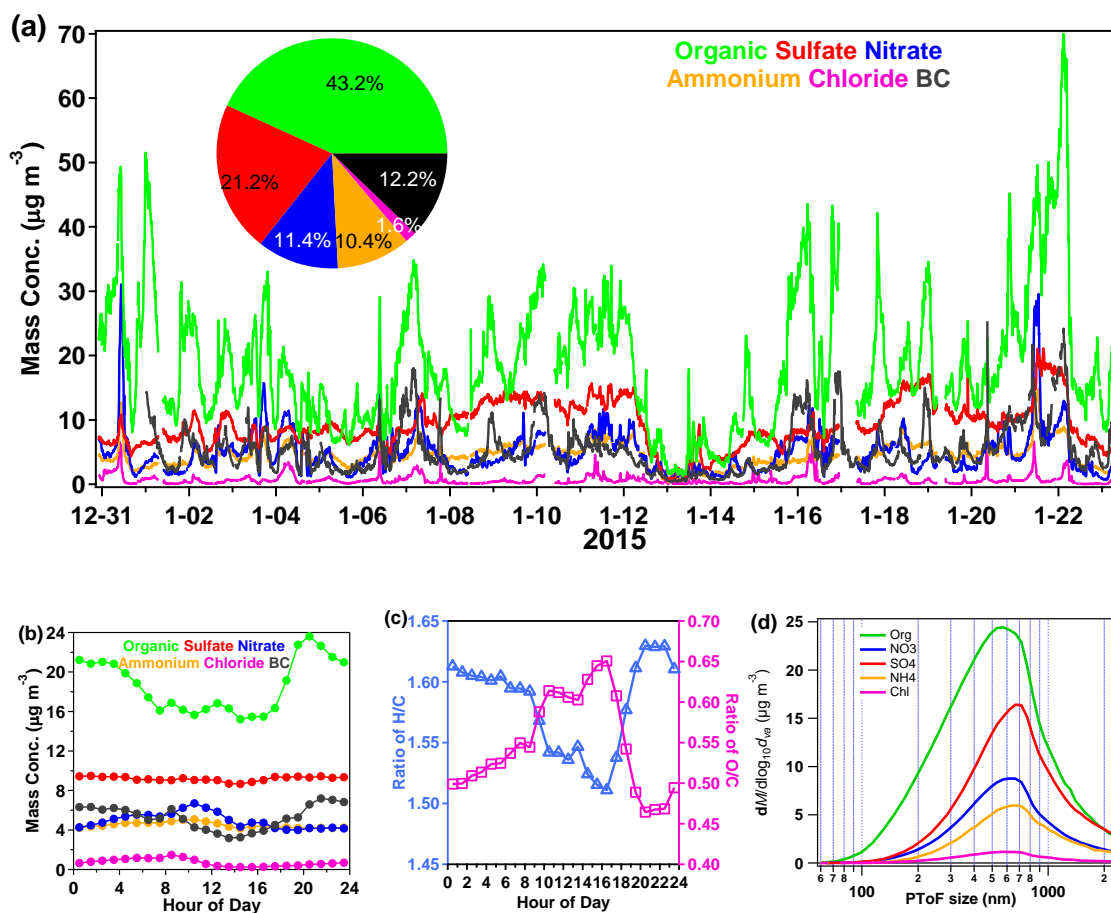
The diurnal variation of the PM$_1$ species in figure 2b shows the average trend during the day. The two peaks in the diurnal
5 variation of BC match the traffic time in the morning at approximately 8:00 and the activity of heavy duty vehicles in the evening. Nitrate showed a significant peak shortly after the first peak of BC, indicating the photochemical oxidization of NOx emitted by vehicles. Then, the concentration of nitrate decreased because of the lifting of the planetary boundary layer (PBL), and then later, nitrate increased again slightly due to the enhancement of sunlight at 14:00. The gas-particle phase partitioning of semi-volatile NH$_4$Cl with the variation of ambient temperature and the height of the PBL can be the crucial factor that
10 caused the diurnal trend of chloride. Sulfate is a less-volatile species, so it would not be significantly evaporated, thus losing particulate mass, with increasing ambient temperature. Sulfate showed a slightly variation, which was mainly affected by the vertical fluctuation of the PBL during the day, which implies that sulfate was mostly a regional product of oxidation by SO$_2$ that is transported on a large regional scale (Salcedo et al., 2006). The mass concentration of ammonium can be regarded as the combination of sulfate, nitrate and chloride based on the neutralization of cations and anions, so the diurnal variation of
15 ammonium was influenced by sulfate, nitrate and chloride. Organics are a much more complex mixture of many different types of organic components that are emitted and produced by various primary and secondary sources. As shown in figure 2b, the diurnal variation of organics showed three peaks, as they were influenced by many different factors, which will be discussed in Section 3.3.

The average O/C ambient value is 0.52, which is higher than the lowest O/C (avg. 0.4) of OAs in urban environments but
20 lower than the average O/C (0.7) in remote/rural environments, while the average H/C ratio (1.61) is lower than that in urban environments (1.7) but higher than that in remote/rural environments (1.5) (Chen et al., 2015). The diurnal variations of O/C plotted in figure 2c show a good correlation with the temperature variation during the day, while H/C shows the opposite trend, indicating the oxidation process of OAs in the atmosphere. Additionally, the H/C ratio shows a small peak at approximately 13:00 to 14:00, which may be due to the fact that some primary organic aerosols were emitted around noon, mostly by cooking
25 activities, as discussed in section 3.3.

Figure 2d shows the average size distribution of the five non-refractory species measured by the AMS. The peaks of all the species were at approximately 500 – 700 nm in the accumulation modes, indicating that the aerosols had been aged in the atmosphere (Alfarra et al., 2004; Zhang et al., 2005). The inorganic aerosol species showed a similar average size distribution during the experiment as described in previous studies in Shenzhen (He et al., 2011), which may be caused by the internal
30 mixing and similar gas-particle distribution processes. The peak of organics was at a smaller size compared to other species, with a much broader size distribution at smaller sizes, which means that both primary emissions and products of photochemical reactions of VOCs have a significant influence on the organic pollution. The peak of sulfate was larger in size than those of

the other four species, and the size distribution of sulfate showed an apparent tendency towards a larger size, implying that sulfate was more aged in the air and most probably had been transported regionally.

Figure 2. (a) Time series and the mass percentages of PM$_1$ composition; (b) diurnal variation of PM$_1$ species; (c) diurnal variation of H/C ratio and O/C ratio; (d) average size distribution of non-refractory PM$_1$ species.

3.2 Volatility of PM$_1$ species

Figure 3 shows the mass fraction remaining (MFR) of the non-refractory species measured by the AMS. The MFR is calculated as the ratio of the species mass concentration (measured with pre-processing by the TD at different temperatures) to the mass concentration measured directly by the AMS. The negative and dispersed points were removed from the calculation of average MFRs. The narrow average MFR ± standard deviation region shows that the volatilities of these species were stable during the measurement. The MFRs of the total non-refractory species and organics all showed nearly linear correlations with the TD temperature, which is consistent with the fact that they consist of various compounds with a wide range of volatilities. For

organics, the MFR was 0.88 at 50 °C, 0.63 at 100 °C, 0.32 at 150 °C and, finally, 0.16 at 200 °C. Based on the linear relationship of the MFR of organics and the TD temperature, the evaporation rate of organics is approximately 0.45% °C^{-1}. Figure 3 also shows the MFRs of inorganic species with different temperature, and all the inorganic species showed trends similar to the results shown by Huffman et al., 2008. Nitrate and chloride show similar trends: they both decreased sharply from ambient

5 temperature to 50 °C, reaching approximately 0.57, and then decreased at a lower rate from 50 to 150 °C, and when the TD temperature increased to 200 °C, the MFRs of nitrate and chloride were at approximately 0.08, lower than those of all the other species. Sulfate is the least volatile species among all PM$_1$ species, and the MFR of sulfate does not show a significant decreasing trend with temperature below 100 °C (0.93 at 50 °C and 0.89 at 100 °C); when the temperature reached 150 °C, the MFR decreased sharply to 0.43, with 11% left at 200 °C, which is consistent with the discussion in Burtscher et al., 2001:

10 sulphuric acid can be distinguished with temperature between 30 and 125 °C, while ammonium sulfate and bisulfate would evaporate with temperature between 125 and 175 °C.

The relationship of O/C ratio with temperature is also shown in figure 3b. It can be seen that the O/C kept increasing as the TD temperature increased, especially when the temperature went from 150 to 200 °C; the O/C increased much more than it did with the temperatures below 150 °C, which is consistent with previous studies (Xu et al., 2016). This can be caused by two

15 factors: (1) species with higher O/C ratios are less volatile, as previous PMF results correlated higher volatility with reduced species and lower volatility with oxygenated species (Ng et al., 2010; Huang et al., 2012); and (2) OA is heated and oxidized to more aged compounds when it goes through the TD, especially when the temperature is higher than 150 °C, and the result is consistent with the OA evolution process (Jimenez et al., 2009).
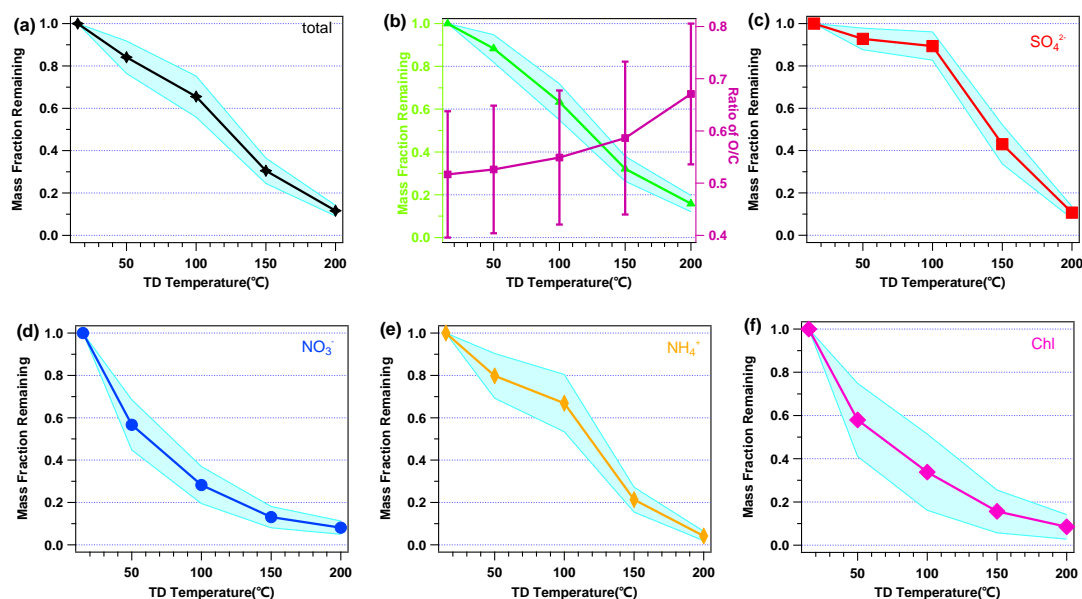
Figure 3. Average mass fraction remaining (MFR) of the total of non-refractory species, organics and inorganic species and the ratio of O/C. The shaded region is the average MFR±standard deviation.

3.3 Source Apportionment

Organics are one of the most important chemical classes/species in aerosol pollution in Shenzhen, contributing 43.2% to the
total PM_1 composition. Because organics are a much more complex class than other species and are emitted by many different
sources, positive matrix factorization (PMF) was conducted based on the high-resolution mass spectra of organics measured
with the HR-ToF-AMS during the experiment, as discussed in section 2.4. The optimal PMF result for the total organic data
measured by the AMS under both ambient temperature and high temperature through the TD is the 5-factor solution with
fpeak=0 and seed=0. Figure 4a shows the MS profiles of the five factors, including a hydrocarbon-like organic aerosol (HOA),
a cooking organic aerosol (COA), a biomass burning organic aerosol (BBOA), a less-oxidized oxygenated organic aerosol
(LO-OOA) and a more-oxidized oxygenated organic aerosol (MO-OOA). As shown in figure 4d, under ambient temperature,
HOA, COA, BBOA LO-OOA and MO-OOA accounted for 13.5%, 20.6%, 8.9%, 39.1% and 17.9% of the total organic mass
on average, respectively.

HOA is most often dominated by long chain hydrocarbon ion series of $C_nH_{2n+1}^+$ and $C_nH_{2n-1}^+$ (Canagaratna et al., 2004; Mohr
et al., 2009; Ng et al., 2010), and the average O/C of HOA was 0.10 in Shenzhen during January 2015, which was similar to
values described in previous publications (Aiken et al., 2009; Huang et al., 2010). Black carbon (BC) is regarded as a tracer of
HOA, and BC can be significantly emitted by primary fuel combustion and biomass burning. The good correlation of HOA
and BC (R^2=0.81) suggested that HOA was mainly from primary fuel combustion, as identified by previous publications
(Zhang et al., 2007a; Lanz et al., 2007; Ulbrich et al., 2009). The diurnal variation of HOA also showed peaks that matched
the traffic time, indicating that traffic emissions are the obvious source of the HOA.

The O/C ratio of COA is 0.18, which is similar to the previous results shown in Mohr et al., 2012. The mass spectral signature
of COA is dominated by the ion series of $C_nH_{2n+1}^+$ and $C_mH_{2m+1}CO^+$ (m/z 29, 43,57,71, 85…), $C_nH_{2n-1}^+$ and $C_mH_{2m-1}CO^+$
(m/z 41, 55, 69, 83…), which are mainly ionized from alkanes, alkenes and, possibly, long chain fatty acids, and COA is
characterized by ions of m/z 41 (mainly $C_3H_5^+$) and m/z 55 (mainly $C_4H_7^+$ and $C_3H_5O^+$) (He et al., 2010; Huang et al., 2010;
Mohr et al., 2009; Mohr et al., 2012). Mohr et al., 2012 also identified COA from HOA by comparing the signals of m/z 55
and m/z 57 and determined that the differentiation between COA and HOA is mainly driven by the oxygen-containing ions of
$C_3H_3O^+$ and $C_3H_5O^+$; especially if the signal ratio of m/z 55 to m/z 57 is larger than 2, it probably can be recognized as COA.
The diurnal variation of COA in Figure 4c shows a small peak at approximately 8:00 am, breakfast time, and the second peak
at approximately 14:00 corresponds with lunch time. The mass concentration of COA also rises after 17:00, which is the time
for dinner and partly because of the decreasing PBL height. The good correlation of COA with the tracer ion $C_6H_{10}O$ (R^2=0.91)
(Sun et al., 2011; Crippa et al., 2013; Elser et al., 2016) also demonstrated the presence of COA.

The most abundant signals in BBOA are m/z 29 (CHO^+) and m/z 43 ($C_2H_3O^+$), and there are more fragments in the range of m/z > 100 for BBOA than for COA and HOA (He et al., 2010). BBOA can be identified by the contribution of m/z 60 (mostly $C_2H_4O_2^+$), which is distinct fragment of ionized levoglucosan, the molecular marker of wood burning and biomass burning (Alfarra et al., 2007; Aiken et al., 2009; Mohr et al., 2009). Some previous studies have shown that the background level of

5   m/z 60 /OA is approximately 0.3% in urban areas without biomass burning impacts (DeCarlo et al., 2008; Docherty et al., 2008). The signal of m/z 60 in BBOA is 1.36% in this study, indicating the presence of BBOA during this experiment, and the BBOA correlated well with m/z 60 (R^2=0.83). The O/C ratio of BBOA in this study is 0.33. It varied across a wide range in previous laboratory and field studies; e.g., He et al., 2010 reported an O/C from 0.18 to 0.26 for six types of biomass burning emissions, and the O/C for lodgepole pine and sage/rabbitbrush burning were 0.31 and 0.42, reported by Aiken et al., 2008.

10   Aiken et al., 2009 and Decarlo et al., 2010 reported O/C values of 0.30 and 0.42 for ambient aerosols, respectively. The BBOA identified in Shenzhen by He et al., 2011 had an O/C of 0.32 and showed a similar diurnal trend as this study, indicating the significant influence that BBOA has on the atmospheric aerosol pollution in Shenzhen.

OOA is recognized by the most intense signal of m/z 44 (CO_2^+), and the signals at higher values of m/z are lower relative to those of other OA factors; furthermore, the OOA can be divided into two factors, the less-oxygenated OOA (LO-OOA,

15   typically named semi-volatile OOA) and the more-oxygenated OOA (MO-OOA, typically named less-volatile OOA), according to the O/C ratios and f44 (Jimenez et al., 2009; Ng et al., 2010; Xu et al., 2015). The factor with a relatively higher O/C ratio (= 0.95) of OOA and significantly higher f44 than f43 is identified as MO-OOA; it showed a good correlation (R^2=0.64) with sulfate, which was also more aged, less volatile and probably had been transported regionally. Meanwhile, LO-OOA, which is less oxygenated (O/C = 0.76), showed a good correlation with nitrate (R^2=0.46) and a narrow gap between f43

20   and f44. The diurnal variations of both LO-OOA and MO-OOA showed higher concentrations during the daytime, denoting their secondary nature. The diurnal variation of MO-OOA was relatively stable compared to that of LO-OOA, which is consistent with that MO-OOA is a more aged and regional component. The contribution of the two OOAs to total OAs is 57.0%, indicating that OOA contributes the majority of the OA pollution in wintertime in Shenzhen.

Atmospheric
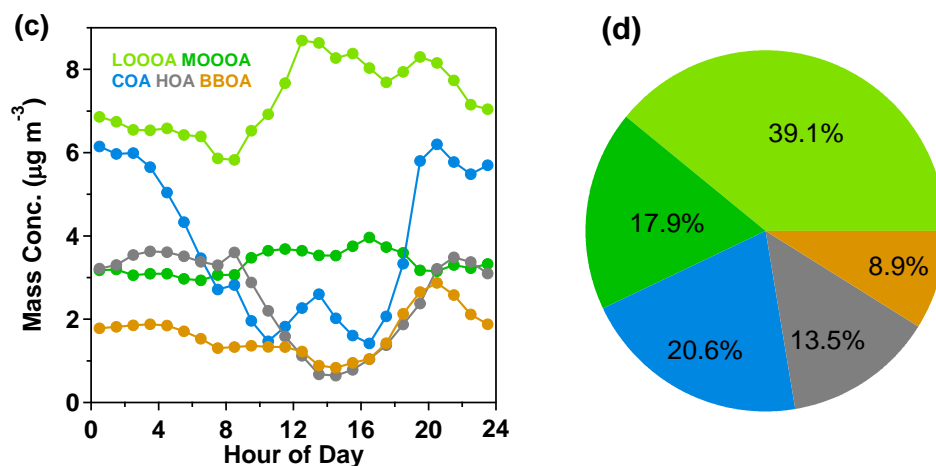Chemistry
and Physics
Discussions
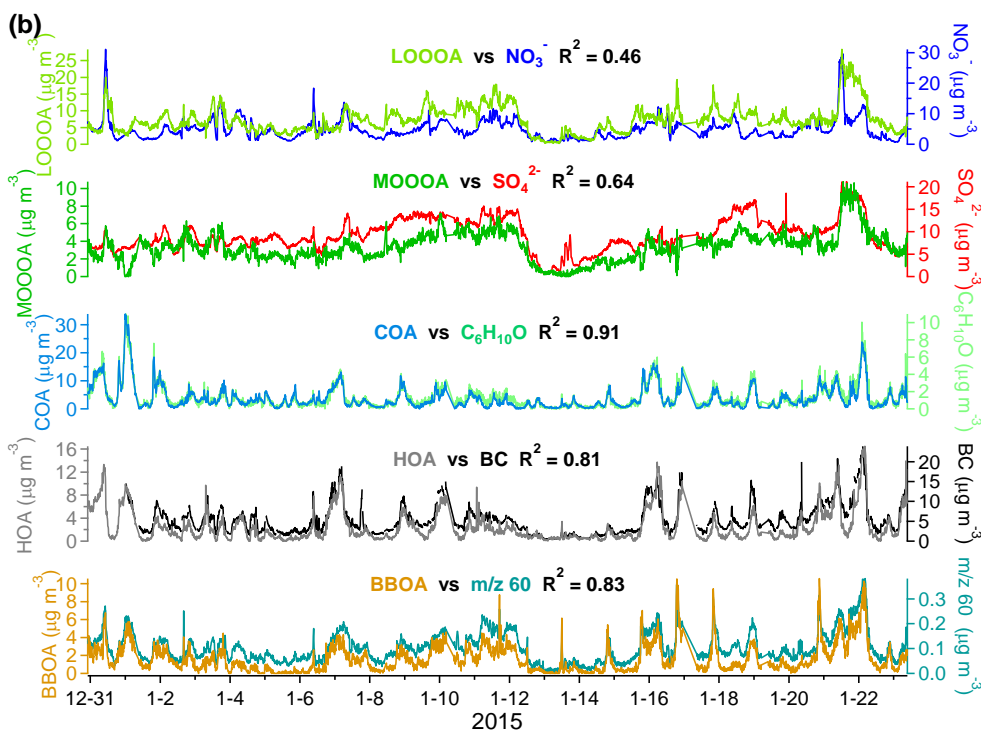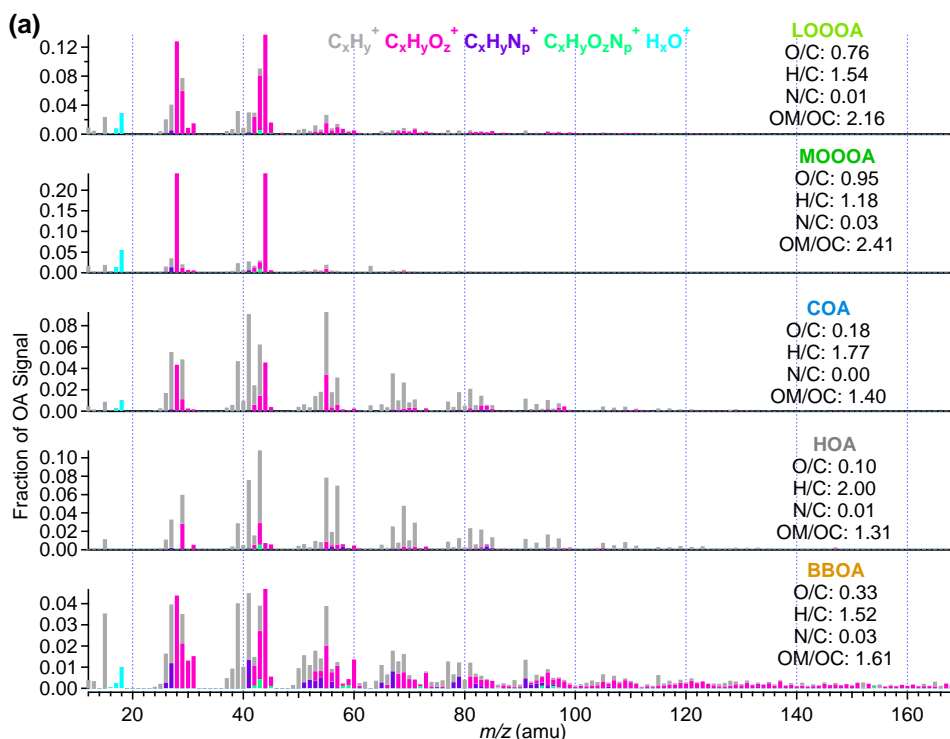
Figure 4 (a) MS profiles of the five OA factors identified by PMF; (b) time series of the five OA factors and the correlation with the relevant species during the experiment; (c) the diurnal variation of the five OA factors; (d) the average contributions of the five OA factors to total OAs. The time series, diurnal variation and pie chart display the results from ambient data.

3.4 Volatility of OA factors

Figure 5a shows the MFR of HOA. The MFR is 0.56 at 50 °C. The MFR of HOA decreases by 1.26 %·°C^{-1} from ambient temperature to 50 °C, and only ~17.8% remains at 100 °C. Then, the evaporation rate slows down significantly, with 7.6% left at 200 °C. Previous dilution sampling studies using a conventional two-product model also demonstrated that both traffic exhaust and wood smoke contain semi-volatile species (Shrivastava et al., 2006). Huffman et al., 2009b also determined that HOA appeared to be more volatile than OOAs.

BBOA showed significant volatility in this study. The evaporation rate (0.37%·°C^{-1}) of BBOA near ambient temperature, with an MFR of 0.87 at 50 °C, in this study is close to that of the least volatile BBOA (0.2%·°C^{-1}) in Huffman et al., 2009a. The volatility of BBOA varied greatly based on the kinds of wood and combustion conditions; it can be very high according to the studies of Aiken et al., 2009 and Huffman et al., 2009a, and can also be very low, as the BBOA from sage and rabbitbrush burning is the least-volatile OA detected by a TD-AMS (Huffman et al., 2009a).

COA also showed similar volatility, with an MFR of 0.85 at 50 °C and 15.0% remaining at 200 °C, higher than those of both HOA and BBOA. This is consistent with previous studies, which recognized that COA is dominated by fatty acids, which have low volatility, evaporated at high cooking temperatures and condensed after cooling down to ambient temperature (Mohr et al., 2009). The evaporation rate of COA is approximately 0.44%·°C^{-1} near ambient temperature, slower compared to the results of meat-cooking OAs shown in Huffman et al., 2009a.

12

The volatility of LO-OOA (MFR of 0.70 at 50 °C) is higher than those of COA, BBOA and MO-OOA (MFR of 0.99 at 50 °C) but lower than that of HOA. Among the five factors, MO-OOA can be regarded as the least volatile species; the MFR curve remained stable at 50 °C and decreased slowly with increasing temperature. The MFR was still at 51.5% even when the temperature in the TD reached 200 °C. The OOA here is the combination of LO-OOA and MO-OOA. The MFR curve of

5   OOA in this study shows a similar decreasing trend as the OOA in winter in Paris (Paciga et al., 2016). OOA is regarded as a good surrogate of SOA, and it showed a relatively good linear correlation, with an evaporation rate of 0.54 %·°C^{-1} at temperatures under 150 °C.

According to the comparison of the volatilities of the five OA factors, the rough sequence of the volatility for different OAs should be summarized as HOA < LO-OOA < BBOA ≈ COA< MO-OOA. As the most volatile species, HOA can be

10   evaporated easily and/or transformed to less volatile OOA through "Evaporation – Oxidation in gas phase - Condensation" as the oxidation processes of HOA to SV-OOA and LV-OOA described in Huang et al., 2012 and the evolution of OA discussed by Jimenez et al., 2009. Therefore, it is difficult to resolve HOA in downwind regions far from urban and industrial areas (Huang et al., 2011; Zhu et al., 2016). Previous studies also showed that semi-volatile hydrocarbons from diesel exhaust (Robinson et al., 2007) and crude oil (de Gouw et al., 2011) can also be easily oxidized to SOA. Therefore, not only the

15   oxidation of VOCs but also the oxidation of HOA can probably be an important source of SOA based on the nature of volatility of HOA. BBOA and COA showed less volatility compared to LO-OOA, suggesting that their ageing could not be a significant source of LO-OOA.
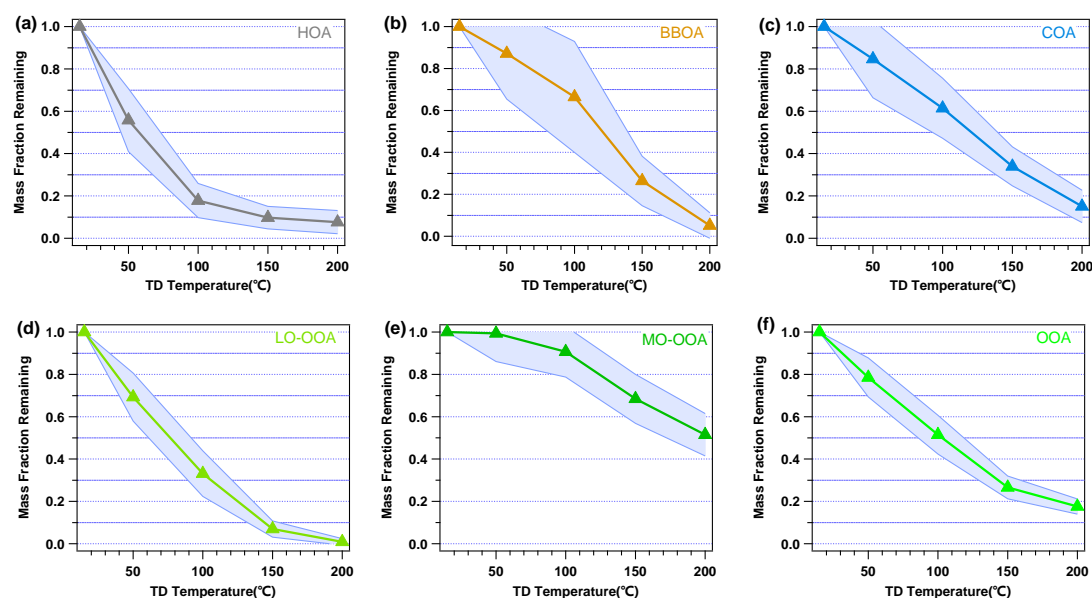
20   **Figure 5 Average mass fraction remaining (MFR) of the five OA factors and OOA (calculated as the combination of MO-OOA and LO-OOA). The shaded region is the average MFR±standard deviation.**

4. Conclusions

The source apportionment and volatility of the PM_1 chemical composition during winter in Shenzhen were investigated based on the TD-AMS system. The mean PM_1 mass concentration was 42.7 ± 20.1 μg m^{-3} during the experiment, with organics (accounting for 43.2%) as the most abundant species. Sulfate, black carbon, nitrate, ammonium and chloride contributed 21.2%, 12.2%, 11.4%, 10.4% and 1.6% to the total PM_1, respectively. The chemical species in PM_1 exhibited a range of volatilities. Nitrate showed the highest volatility among the five species measured with the lowest MFR (0.57) at 50 °C. Organics exhibited a relatively linear MFR decrease, with a rate of 0.45 %·°C^{-1}, as the TD temperature increased from ambient to 200 °C, which is mainly due to the complex composition of organics in the atmosphere. The organics were grouped into five subtypes by the PMF analysis, including primarily emitted hydrocarbon-like OA (HOA), cooking OA (COA), biomass burning OA (BBOA) and two secondarily formed oxygenated OAs: a less-oxygenated OOA (LO-OOA) and a more-oxygenated OOA (MO-OOA), and they accounted for 13.5%, 20.6%, 8.9%, 39.1% and 17.9% of the total OAs, respectively. Among all the five OA factors, HOA was the most volatile species, whereas MO-OOA had the lowest volatility with the slowest evaporation rate. According to the MFR of different OA factors at 50 °C, the volatility sequence of the five OA factors should be HOA (MFR of 0.56 at 50 °C) > LO-OOA (0.70) > COA (0.85) ≈ BBOA (0.87) > MO-OOA (0.99), which implied that HOA, rather than BBOA or COA, could be a potentially important source of LO-OOA.

Acknowledgments

References

Aiken, A. C., Decarlo, P. F., Kroll, J. H., Worsnop, D. R., Huffman, J. A., Docherty, K. S., Ulbrich, I. M., Mohr, C., Kimmel, J. R., Sueper, D., Sun, Y., Zhang, Q., Trimborn, A., Northway, M., Ziemann, P. J., Canagaratna, M. R., Onasch, T. B., Alfarra, M. R., Prevot, A. S. H., Dommen, J., Duplissy, J., Metzger, A., Baltensperger, U., and Jimenez, J. L.: O/C and OM/OC ratios of primary, secondary, and ambient organic aerosols with high resolution time-of-flight aerosol mass spectrometry, Environ. Sci. Technol., 42, 4478–4485, doi:10.1021/es703009q, 2008.

Aiken, A. C., Salcedo, D., Cubison, M. J., Huffman, J. A., DeCarlo, P. F., Ulbrich, I. M., Docherty, K. S., Sueper, D., Kimmel, J. R., Worsnop, D. R., Trimborn, A., Northway, M., Stone, E. A., Schauer, J. J., Volkamer, R. M., Fortner, E., de Foy, B., Wang, J., Laskin, A., Shutthanandan, V., Zheng, J., Zhang, R., Gaffney, J., Marley, N. A., Paredes-Miranda, G., Arnott, W. P., Molina, L. T., Sosa, G., and Jimenez, J. L.: Mexico City aerosol analysis during MILAGRO using high resolution aerosol mass spectrometry at the urban supersite (T0) – Part 1: Fine particle composition and organic source apportionment, Atmos. Chem. Phys., 9, 6633-6653, doi:10.5194/acp-9-6633-2009, 2009.

Alfarra, M. R., Coe, H., Allan, J. D., Bower, K. N., Boudries, H., Canagaratna, M. R., Jimenez, J. L., Jayne, J. T., Garforth, A. A., Li, S. M., and Worsnop, D. R.: Characterization of urban and rural organic particulate in the lower fraser valley using two aerodyne aerosol mass spectrometers. Atmos. Environ, 38(34), 5745-5758, doi:10.1016/j.atmosenv.2004.01.054, 2004.

5   Alfarra, M. R., Prevot, A. S., Szidat, S., Sandradewi, J., Weimer, S., Lanz, V. A., Schreiber, D., Mohr, M., and Baltensperger, U.: Identification of the mass spectral signature of organic aerosols from wood burning emissions. Environ. Sci. Technol, 41(16), 5770-5777, doi:10.1021/es062289b, 2007.

An, W. J., Pathak, R. K., Lee, B. H., and Pandis, S. N.: Aerosol Volatility Measurement Using an Improved Thermodenuder: Application to Secondary Organic Aerosol. J. Aerosol Sci., 38:305–314, doi:10.1016/j.jaerosci.2006.12.002, 2007.

10 Baklanov, A., Molina, L.T., Gauss, M.: Megacities, air quality and climate. Atmos. Environ. 126, 235–249, doi:10.1016/j.atmosenv.2015.11.059, 2015.

Bi, X., Dai, S., Zhang, G., Qiu, N., Li, M., Wang, X., Chen, D., Peng, P., Sheng, G., Fu, J., and Zhou, Z.: Real-time and single-particle volatility of elemental carbon-containing particles in the urban area of pearl river delta region, china. Atmos. Environ., 118(1), 194-202, doi:10.1016/j.atmosenv.2015.08.012, 2015.

15 Bidleman, T. F.: Atmospheric processes: wet and dry deposition of organic compounds are controlled by their vapor-particle partitioning. Environ. Sci. Technol., 22(4), 361-367, doi:10.1021/es00169a002, 1988.

Bohnenstengel, S. I., Belcher, S. E., Aiken, A., Allan, J. D., Allen, G., Bacak, A., Bannan, T. J., Barlow, J. F., Beddows, D. C. S., Bloss, W. J., Booth, A. M., Chemel, C., Coceal, O., Di Marco, C. F., Dubey, M. K., Faloon, K. H., Fleming, Z. L., Furger, M., Gietl, J. K., Graves, R. R., Green, D. C., Grimmond, C. S. B., Halios, C. H., Hamilton, J. F., Harrison, R. M.,
20 Heal, M. R., Heard, D. E., Helfter, C., Herndon, S. C., Holmes, R. E., Hopkins, J. R., Jones, A. M., Kelly, F. J., Kotthaus, S., Langford, B., Lee, J. D., Leigh, R. J., Lewis, A. C., Lidster, R. T., Lopez-Hilfiker, F. D., McQuaid, J. B., Mohr, C., Monks, P. S., Nemitz, E., Ng, N. L., Percival, C. J., Prévôt, A. S. H., Ricketts, H. M. A., Sokhi, R., Stone, D., Thornton, J. A., Tremper, A. H., Valach, A. C., Visser, S., Whalley, L. K., Williams, L. R., Xu, L., Young, D. E., and Zotter, P.: Meteorology, Air Quality, and Health in London: The ClearfLo Project, B. Am. Meteorol. Soc., 96, 779–804,
25 doi:10.1175/BAMS-D-12-00245.1, 2014.

Boman, C., Nordin, A., Westerholm, R., and Pettersson, E.: Evaluation of a constant volume sampling setup for residential biomass fired appliances—influence of dilution conditions on particulate and pah emissions. Biomass. Bioenergy., 29(4), 258-268, doi.org/10.1016/j.biombioe.2005.03.003, 2005.

Burtscher, H., Baltensperger, U., Bukowiecki, N., Cohn, P., Hüglin, C., Mohr, M., Matter, U., Nyeki, S., Schmatloch, V.,
30 Streit, N., and Weingartner, E.: Separation of volatile and non-volatile aerosol fractions by thermodesorption: instrumental development and applications. J. Aerosol Sci., 32(4), 427-442, doi:10.1016/S0021-8502(00)00089-6, 2001.

Canagaratna, M.R., Jayne, J.T., Ghertner, D.A., Herndon, S., Shi, Q., Jimenez, J.L., Silva, P. J., Williams, P., Lanni, T., Drewnick, F., Demerjian, K. L., Kolb, C. E., and Worsnop, D. R.: Chase studies of particulate emissions from in-use New York City vehicles. Aerosol Sci. Technol. 38 (6), 555–573, doi:10.1080/02786820490465504, 2004.

Canagaratna, M.R., Jayne, J.T., Jimenez, J.L., Allan, J.D., Alfarra, M.R., Zhang, Q., Onasch, T. B., Drewnick, F., Coe, H., Middlebrook, A., Delia, A., Williams, L. R., Trimborn, A. M., Northway, M. J., DeCarlo, P. F., Kolb, C. E., Davidovits, P., Worsnop, D. R.: Chemical and microphysical characterization of ambient aerosols with the aerodyne aerosol mass spectrometer. Mass. Spectrom. Rev. 26 (2), 185–222, doi:10.1002/mas.20115, 2007.

5   Chen, Q., Heald, C. L., Jimenez, J. L., Canagaratna, M. R., Zhang, Q., He, L., Huang, X., Campuzano-Jost, P., Palm, B. B., Poulain, L., Kuwata, M., Martin, S. T., Abbatt, J. P .D., Lee, A. K. Y., and Liggio, J.: Elemental composition of organic aerosol: the gap between ambient and laboratory measurements. Geophys. Res. Lett. 42(10), 4182-4189, doi:10.1002/2015GL063693, 2015.

Crippa, M., Haddad, I. E., Slowik, J. G., Decarlo, P. F., Mohr, C., Heringa, M. F., Chirico, R., Marchand, N., Sciare, J.,
10   Baltensperger, U., and Prevot, A. S. H.: Identification of marine and continental aerosol sources in Paris using high resolution aerosol mass spectrometry. J. Geophys. Res. Atmos. 118(4), 1950-1963, doi:10.1002/jgrd.50151, 2013.

de Gouw, J. A. D., Middlebrook, A. M., Warneke, C., Ahmadov, R., Atlas, E. L., Bahreini, R., Blake, D. R., Brock, C. A., Brioude, J., Fahey, D. W., Fehsenfeld, F. C., Holloway, J. S., Le Henaff, M., Lueb, R. A., McKeen, S. A., Meagher, J. F., Murphy, D. M., Paris, C., Parrish, D. D., Perring, A. E., Pollack, I. B., Ravishankara, A. R., Robinson, A. L., Ryerson, T.
15   B., Schwarz, J. P., Spackman, J. R., Srinivasan, A., and Watts, L. A.: Organic aerosol formation downwind from the deepwater horizon oil spill. Science, 331, 1295-1299, doi:10.1126/science.1200320, 2011.

DeCarlo, P. F., Dunlea, E. J., Kimmel, J. R., Aiken, A. C., Sueper, D., Crounse, J., Wennberg, P. O., Emmons, L., Shinozuka, Y., Clarke, A., Zhou, J., Tomlinson, J., Collins, D. R., Knapp, D., Weinheimer, A. J., Montzka, D. D., Campos, T., and Jimenez, J. L.: Fast airborne aerosol size and chemistry measurements above Mexico City and Central Mexico during the
20   MILAGRO campaign, Atmos. Chem. Phys., 8, 4027-4048, doi:10.5194/acp-8-4027-2008, 2008.

DeCarlo, P. F., Ulbrich, I. M., Crounse, J., de Foy, B., Dunlea, E. J., Aiken, A. C., Knapp, D., Weinheimer, A. J., Campos, T., Wennberg, P. O., and Jimenez, J. L.: Investigation of the sources and processing of organic aerosol over the Central Mexican Plateau from aircraft measurements during MILAGRO, Atmos. Chem. Phys., 10, 5257-5280, doi:10.5194/acp-10-5257-2010, 2010.

25   Decarlo, P.F., Kimmel, J.R., Trimborn, A, Northway, M.J., Jayne, J.T., Aiken, A.C., Gonin, M., Fuhrer, K., Horvath, T., Docherty, K. S., Worsnop, D. R., and Jimenez, J. L.: Field-deployable, high-resolution, time-of-flight aerosol mass spectrometer. Anal. Chem. 78 (24), 8281–8289, doi:10.1021/ac061249n, 2006.

Docherty, K. S., Stone, E. A., Ulbrich, I. M., Decarlo, P. F., Snyder, D. C., Schauer, J. J., Peltier, R. E., Weber, R. J., Murphy, S. M., Seinfeld, J. H., Grover, B. D., Eatough, D. J., and Jimenez, J. L.: Apportionment of primary and secondary organic
30   aerosols in southern california during the 2005 study of organic aerosols in riverside (SOAR-1). Environ. Sci. Technol, 42(20), 7655-7662, doi:10.1021/es8008166, 2008.

Donahue, N.M., Robinson, A. L., Stanier, C. O., and Pandis, S., N.: Coupled Partitioning, Dilution, and Chemical Aging of Semivolatile Organics. Environ. Sci. Technol., 40:2635–2643, doi:10.1021/es052297c, 2006.

Elser, M., Huang, R.-J., Wolf, R., Slowik, J. G., Wang, Q., Canonaco, F., Li, G., Bozzetti, C., Daellenbach, K. R., Huang, Y., Zhang, R., Li, Z., Cao, J., Baltensperger, U., El-Haddad, I., and Prévôt, A. S. H.: New insights into PM2.5 chemical composition and sources in two major cities in China during extreme haze events using aerosol mass spectrometry, Atmos. Chem. Phys., 16, 3207-3225, doi:10.5194/acp-16-3207-2016, 2016.

5 Feng, J., Hu, M., Chan, C. K., Lau, P. S., Fang, M., He, L., and Tang X.: A comparative study of the organic matter in pm2.5 from three Chinese megacities in three different climatic zones. Atmos. Environ., 40(21), 3983-3994, doi:10.1016/j.atmosenv.2006.02.017, 2006.

Faulhaber, A. E., Thomas, B. M., Jimenez, J. L., Jayne, J. T., Worsnop, D. R., and Ziemann, P. J.: Characterization of a thermodenuder-particle beam mass spectrometer system for the study of organic aerosol volatility and composition,
10   Atmos. Meas. Tech., 2, 15-31, doi:10.5194/amt-2-15-2009, 2009.

Hallquist, M., Wenger, J. C., Baltensperger, U., Rudich, Y., Simpson, D., Claeys, M., Dommen, J., Donahue, N. M., George, C., Goldstein, A. H., Hamilton, J. F., Herrmann, H., Hoffmann, T., Iinuma, Y., Jang, M., Jenkin, M. E., Jimenez, J. L., Kiendler-Scharr, A., Maenhaut, W., McFiggans, G., Mentel, Th. F., Monod, A., Prévôt, A. S. H., Seinfeld, J. H., Surratt, J. D., Szmigielski, R., and Wildt, J.: The formation, properties and impact of secondary organic aerosol: current and
15   emerging issues, Atmos. Chem. Phys., 9, 5155–5236, doi:10.5194/acp-9-5155-2009, 2009.

He, L.-Y., Lin, Y., Huang, X.-F., Guo, S., Xue, L., Su, Q., Hu, M., Luan, S.-J., and Zhang, Y.-H.: Characterization of high-resolution aerosol mass spectra of primary organic aerosol emissions from Chinese cooking and biomass burning, Atmos. Chem. Phys., 10, 11535-11543, doi:10.5194/acp-10-11535-2010, 2010.

He, L., Huang, X., Xue, L., Hu, M., Lin, Y., & Zheng, J., Zhang, R., and Zhang, Y.: Submicron aerosol analysis and organic
20   source apportionment in an urban atmosphere in pearl river delta of china using high‐resolution aerosol mass spectrometry. J. Geophys. Res. Atmos., 116(D12), 1248-1256, doi:10.1029/2010JD014566, 2011.

Hu, W., Palm, B. B., Day, D. A., Campuzano-Jost, P., Krechmer, J. E., Peng, Z., de Sá, S. S., Martin, S. T., Alexander, M. L., Baumann, K., Hacker, L., Kiendler-Scharr, A., Koss, A. R., de Gouw, J. A., Goldstein, A. H., Seco, R., Sjostedt, S. J., Park, J.-H., Guenther, A. B., Kim, S., Canonaco, F., Prévôt, A. S. H., Brune, W. H., and Jimenez, J. L.: Volatility and
25   lifetime against OH heterogeneous reaction of ambient isoprene-epoxydiols-derived secondary organic aerosol (IEPOX-SOA), Atmos. Chem. Phys., 16, 11563-11580, doi:10.5194/acp-16-11563-2016, 2016.

Hu, W., Campuzano-Jost, P., Day, D. A., Croteau, P., Canagaratna, M. R., Jayne, J. T., Worsnop, D. R., and Jimenez, J. L.: Evaluation of the new capture vaporizer for aerosol mass spectrometers (ams) through field studies of inorganic species. Aerosol Science & Technology, 1-55, doi.org/10.1080/02786826.2017.1296104, 2017.

30 Huang, X.-F., He, L.-Y., Hu, M., Canagaratna, M. R., Sun, Y., Zhang, Q., Zhu, T., Xue, L., Zeng, L.-W., Liu, X.-G., Zhang, Y.-H., Jayne, J. T., Ng, N. L., and Worsnop, D. R.: Highly time-resolved chemical characterization of atmospheric submicron particles during 2008 Beijing Olympic Games using an Aerodyne High-Resolution Aerosol Mass Spectrometer, Atmos. Chem. Phys., 10, 8933-8945, doi:10.5194/acp-10-8933-2010, 2010.

Huang, X.-F., He, L.-Y., Hu, M., Canagaratna, M. R., Kroll, J. H., Ng, N. L., Zhang, Y.-H., Lin, Y., Xue, L., Sun, T.-L., Liu, X.-G., Shao, M., Jayne, J. T., and Worsnop, D. R.: Characterization of submicron aerosols at a rural site in Pearl River Delta of China using an Aerodyne High-Resolution Aerosol Mass Spectrometer, Atmos. Chem. Phys., 11, 1865-1877, https://doi.org/10.5194/acp-11-1865-2011, 2011.

Huang, X.-F., He, L.-Y., Xue, L., Sun, T.-L., Zeng, L.-W., Gong, Z.-H., Hu, M., and Zhu, T.: Highly time-resolved chemical characterization of atmospheric fine particles during 2010 Shanghai World Expo, Atmos. Chem. Phys., 12, 4897-4907, doi:10.5194/acp-12-4897-2012, 2012.

Huang, X. F., Xue, L., Tian, X. D.,Shao,W. W.,Sun, T. L., Gong, Z. H., Ju, W-W., Jiang, B., Hu, M., and He, L. Y.: Highly time-resolved carbonaceous aerosol characterization in Yangtze River Delta of China: composition, mixing state and secondary formation. Atmos. Environ. 64, 200–207, doi:10.1016/j.atmosenv.2012.09.059, 2013.

Huffman, J. A., Ziemann, P. J., Jayne, J. T., Worsnop, D. R., and Jimenez, J. L.: Development and characterization of a fast-stepping/scanning thermodenuder for chemically-resolved aerosol volatility measurements. Aerosol Sci. Technol. 42(5), 395-407, doi:10.1080/02786820802104981, 2008.

Huffman, J. A., Docherty, K. S., Mohr, C., Cubison, M. J., Ulbrich, I. M., Ziemann, P. J., Onasch, T. B., and Jimenez, J. L.: Chemically-resolved volatility measurements of organic aerosol from different sources. Environ. Sci. Technol. 43(14), 5351-5357, doi:10.1021/es803539d, 2009a.

Huffman, J. A., Docherty, K. S., Aiken, A. C., Cubison, M. J., Ulbrich, I. M., DeCarlo, P. F., Sueper, D., Jayne, J. T., Worsnop, D. R., Ziemann, P. J., and Jimenez, J. L.: Chemically-resolved aerosol volatility measurements from two megacity field studies, Atmos. Chem. Phys., 9, 7161-7182, doi:10.5194/acp-9-7161-2009, 2009.

IPCC: Climate Change: The Physical Science Basis – Contribution of Working Group I to the Fifth Assessment Report of the Intergovernmental Panel on Climate Change, edited by: Stocker, T. F., Qin, D., Plattner, G. K., Tignor, M., Allen, S. K., Boschung, J., Nauels, A., Xia, Y., Bex, V., and Midgley, P. M., Cambridge University Press, Cambridge, United Kingdom and New York, NY, USA, 1535 pp., 2013.

Jimenez, J. L., Canagaratna, M. R., Donahue, N. M., Prevot, A. S. H., Zhang, Q., Kroll, J. H., DeCarlo, P. F., Allan, J. D., Coe, H., Ng, N. L., Aiken, A. C., Docherty, K. S., Ulbrich, I. M., Grieshop, A. P., Robinson, A. L., Duplissy, J., Smith, J. D., Wilson, K. R., Lanz, V. A., Hueglin, C., Sun, Y. L., Tian, J., Laaksonen, A., Raatikainen, T., Rautiainen, J., Vaattovaara, P., Ehn, M., Kulmala, M., Tomlinson, J. M., Collins, D. R., Cubison, M. J., Dunlea, E. J., Huffman, J. A., Onasch, T. B., Alfarra, M. R., Williams, P. I., Bower, K., Kondo, Y., Schneider, J., Drewnick, F., Borrmann, S., Weimer, S., Demerjian, K., Salcedo, D., Cottrell, L., Griffin, R., Takami, A., Miyoshi, T., Hatakeyama, S., Shimono, A., Sun, J. Y., Zhang, Y. M., Dzepina, K., Kimmel, J. R., Sueper, D., Jayne, J. T., Herndon, S. C., Trimborn, A. M., Williams, L. R., Wood, E. C., Middlebrook, A. M., Kolb, C. E., Baltensperger, U., and Worsnop, D. R.: Evolution of Organic Aerosols in the Atmosphere, Science, 326, 1525–1529, doi:10.1126/science.1180353, 2009.

Kuwata, M., Zorn, S. R., and Martin, S. T.: Using elemental ratios to predict the density of organic material composed of carbon, hydrogen, and oxygen. Environmental Science & Technology, 46(2), 787-94, doi: 10.1021/es202525q, 2012.

Lanz, V. A., Alfarra, M. R., Baltensperger, U., Buchmann, B., Hueglin, C., and Prévôt, A. S. H.: Source apportionment of submicron organic aerosols at an urban site by factor analytical modelling of aerosol mass spectra, Atmos. Chem. Phys., 7, 1503-1522, doi:10.5194/acp-7-1503-2007, 2007.

Lee, B. H., Kostenidou, E., Hildebrandt, L., Riipinen, I., Engelhart, G. J., Mohr, C., DeCarlo, P. F., Mihalopoulos, N., Prevot, A. S. H., Baltensperger, U., and Pandis, S. N.: Measurement of the ambient organic aerosol volatility distribution: application during the Finokalia Aerosol Measurement Experiment (FAME-2008), Atmos. Chem. Phys., 10, 12149-12160, doi:10.5194/acp-10-12149-2010, 2010.

Mohr, C., Huffman, J. A., Cubison, M. J., Aiken, A.C., Docherty, K.S., Kimmel, J.R., Ulbrich, I. M., Hannigan, M., and Jimenez, J. L.: Characterization of primary organic aerosol emissions from meat cooking, trash burning, and motor vehicles with high-resolution aerosol mass spectrometry and comparison with ambient and chamber observations. Environ. Sci. Technol. 43 (7), 2443–2449, doi:10.1021/es8011518, 2009.

Mohr, C., DeCarlo, P. F., Heringa, M. F., Chirico, R., Slowik, J. G., Richter, R., Reche, C., Alastuey, A., Querol, X., Seco, R., Peñuelas, J., Jiménez, J. L., Crippa, M., Zimmermann, R., Baltensperger, U., and Prévôt, A. S. H.: Identification and quantification of organic aerosol from cooking and other sources in Barcelona using aerosol mass spectrometer data, Atmos. Chem. Phys., 12, 1649-1665, doi:10.5194/acp-12-1649-2012, 2012.

Ng, N. L., Canagaratna, M. R., Zhang, Q., Jimenez, J. L., Tian, J., Ulbrich, I. M., Kroll, J. H., Docherty, K. S., Chhabra, P. S., Bahreini, R., Murphy, S. M., Seinfeld, J. H., Hildebrandt, L., Donahue, N. M., DeCarlo, P. F., Lanz, V. A., Prévôt, A. S. H., Dinar, E., Rudich, Y., and Worsnop, D. R.: Organic aerosol components observed in Northern Hemispheric datasets from Aerosol Mass Spectrometry, Atmos. Chem. Phys., 10, 4625-4641, doi:10.5194/acp-10-4625-2010, 2010.

Paatero, P.: The multilinear engine: a table-driven, least squares program for solving multilinear problems, including the n-way parallel factor analysis model. J. Comput. Graph. Stat. 8(4), 854-888, doi:10.2307/1390831, 1999.

Paatero, P., and Hopke, P. K.: Discarding or downweighting high-noise variables in factor analytic models. Anal. Chim. Acta,490(1), 277-289, doi:10.1016/S0003-2670(02)01643-4, 2003.

Paciga, A., Karnezi, E., Kostenidou, E., Hildebrandt, L., Psichoudaki, M., Engelhart, G. J., Lee, B.-H., Crippa, M., Prévôt, A. S. H., Baltensperger, U., and Pandis, S. N.: Volatility of organic aerosol and its components in the megacity of Paris, Atmos. Chem. Phys., 16, 2013-2023, doi:10.5194/acp-16-2013-2016, 2016.

Pankow, J. F., and Badsanti, K. C.: The Carbon Number-Polarity Grid: A Means to Manage the Complexity of the Mix of Organic Compounds When Modeling Atmospheric Organic Particular Matter. Atmos. Environ., 43:2829–2835, doi:10.1016/j.atmosenv.2008.12.050, 2009.

Poulain, L., Birmili, W., Canonaco, F., Crippa, M., Wu, Z. J., Nordmann, S., Spindler, G., Prévôt, A. S. H., Wiedensohler, A., and Herrmann, H.: Chemical mass balance of 300 °C non-volatile particles at the tropospheric research site Melpitz, Germany, Atmos. Chem. Phys., 14, 10145-10162, https://doi.org/10.5194/acp-14-10145-2014, 2014.

Robinson A. L., Donahue N. M., Shrivastava M, K., Weitkamp E. A., Sage A, M., Grieshop A. P., Lane T. E., Pierce J. R., Pandis S. N.: Rethinking organic aerosols: semivolatile emissions and photochemical aging. Science, 315(5816), 1259-1262, doi: 10.1126/science.1133061, 2007.

Salcedo, D., Onasch, T. B., Dzepina, K., Canagaratna, M. R., Zhang, Q., Huffman, J. A., DeCarlo, P. F., Jayne, J. T., Mortimer, P., Worsnop, D. R., Kolb, C. E., Johnson, K. S., Zuberi, B., Marr, L. C., Volkamer, R., Molina, L. T., Molina, M. J., Cardenas, B., Bernabé, R. M., Márquez, C., Gaffney, J. S., Marley, N. A., Laskin, A., Shutthanandan, V., Xie, Y., Brune, W., Lesher, R., Shirley, T., and Jimenez, J. L.: Characterization of ambient aerosols in Mexico City during the MCMA-2003 campaign with Aerosol Mass Spectrometry: results from the CENICA Supersite, Atmos. Chem. Phys., 6, 925-946, doi:10.5194/acp-6-925-2006, 2006.

Shrivastava, M. K., Lipsky, E. M., Stanier, C. O., and Robinson, A. L.: Modeling semivolatile organic aerosol mass emissions from combustion systems. Environ. Sci. Technol., 40(8), 2671-7, doi:10.1021/es0522231, 2006.

Sun, Y.-L., Zhang, Q., Schwab, J. J., Demerjian, K. L., Chen, W.-N., Bae, M.-S., Hung, H.-M., Hogrefe, O., Frank, B., Rattigan, O. V., and Lin, Y.-C.: Characterization of the sources and processes of organic and inorganic aerosols in New York city with a high-resolution time-of-flight aerosol mass apectrometer, Atmos. Chem. Phys., 11, 1581-1602, doi:10.5194/acp-11-1581-2011, 2011.

Ulbrich, I. M., Canagaratna, M. R., Zhang, Q., Worsnop, D. R., and Jimenez, J. L.: Interpretation of organic components from Positive Matrix Factorization of aerosol mass spectrometric data, Atmos. Chem. Phys., 9, 2891-2918, doi:10.5194/acp-9-2891-2009, 2009.

Wehner, B., Philippin, S., and Wiedensohler, A.: Design and calibration of a thermodenuder with an improved heating unit to measure the size-dependent volatile fraction of aerosol particles. J. Aerosol Sci. 33(7), 1087-1093, doi:10.1016/S0021-8502(02)00056-3, 2002.

Xu, L., Suresh, S., Guo, H., Weber, R. J., and Ng, N. L.: Aerosol characterization over the Southeastern United States using high-resolution aerosol mass spectrometry: spatial and seasonal variation of aerosol composition and sources with a focus on organic nitrates, Atmos. Chem. Phys., 15, 7307-7336, doi:10.5194/acp-15-7307-2015, 2015.

Xu, L., Williams, L. R., Young, D. E., Allan, J. D., Coe, H., Massoli, P., Fortner, E., Chhabra, P., Herndon, S., Brooks, W. A., Jayne, J. T., Worsnop, D. R., Aiken, A. C., Liu, S., Gorkowski, K., Dubey, M. K., Fleming, Z. L., Visser, S., Prévôt, A. S. H., and Ng, N. L.: Wintertime aerosol chemical composition, volatility, and spatial variability in the greater London area, Atmos. Chem. Phys., 16, 1139-1160, doi:10.5194/acp-16-1139-2016, 2016.

Zhang, Q., Worsnop, D. R., Canagaratna, M. R., and Jimenez, J. L.: Hydrocarbon-like and oxygenated organic aerosols in Pittsburgh: insights into sources and processes of organic aerosols, Atmos. Chem. Phys., 5, 3289-3311, doi:10.5194/acp-5-3289-2005, 2005.

Zhang, Q., Jimenez, J. L., Canagaratna, M. R., Allan, J. D., Coe, H., Ulbrich, I., Alfarra, M. R., Takami, A., Middlebrook, A. M., Sun, Y. L., Dzepina, K., Dunlea, E., Docherty, K., De- Carlo, P. F., Salcedo, D., Onasch, T., Jayne, J. T., Miyoshi, T., Shimono, A., Hatakeyama, S., Takegawa, N., Kondo, Y., Schneider, J., Drewnick, F., Borrmann, S., Weimer, S.,

Demerjian, K., Williams, P., Bower, K., Bahreini, R., Cottrell, L., Griffin, R. J., Rautiainen, J., Sun, J. Y., Zhang, Y. M., and Worsnop, D. R.: Ubiquity and dominance of oxygenated species in organic aerosols in anthropogenically-influenced Northern Hemisphere midlatitudes, Geophys. Res. Lett., 34, L13801, doi:10.1029/2007gl029979, 2007a.

Zhang, Q., Jimenez, J. L., Worsnop, D. R. & Canagaratna, M. A Case Study of Urban Particle Acidity and Its Influence on

5   Secondary Organic Aerosol. Environ. Sci. Technol. 41, 3213-3219, doi:10.1021/es061812j, 2007b.

Zhu, Q., He, L.-Y., Huang, X.-F., Cao, L.-M., Gong, Z.-H., Wang, C., Zhuang, X., and Hu, M.: Atmospheric aerosol compositions and sources at two national background sites in northern and southern China, Atmos. Chem. Phys., 16, 10283-10297, https://doi.org/10.5194/acp-16-10283-2016, 2016.